Journal of Hazardous Materials 381 (2020) 121202

Contents lists available at ScienceDirect

Journal of Hazardous Materials

journal homepage: www.elsevier.com/locate/jhazmat

In vitro inhalation bioaccessibility procedures for lead in $PM_{2.5}$ size fraction of soil assessed and optimized by *in vivo-in vitro* correlation

Laijin Zhong[a], Xiaolan Liu[a], Xin Hu[a,*], Yijun Chen[a], Hongwei Wang[b], Hong-zhen Lian[a,*]

[a] State Key Laboratory of Analytical Chemistry for Life Science, School of Chemistry & Chemical Engineering and Centre of Materials Analysis, Nanjing University, Nanjing 210023, PR China

[b] Centre for Translational Medicine and Jiangsu Key Laboratory of Molecular Medicine, Medical School, Nanjing University, Nanjing 210093, PR China

ARTICLE INFO

Editor: Rinklebe Jörg

Keywords:
Lead
Inhalation risk
In vivo inhalation bioavailability
In vitro inhalation bioaccessibility
In vivo-in vitro correlation

ABSTRACT

In order to assess and optimize frequently used *in vitro* inhalation bioaccessibility procedures for heavy metals in the inhalation risk assessment, *in vivo* inhalation bioavailability of Pb in simulated atmosphere fine particles ($PM_{2.5}$) from aging soils spiked with lead compounds and field soils in lead-zinc mining areas was investigated via intranasally instilled experiments with these $PM_{2.5}$ suspensions to mice and Pb bioaccessibility was extracted by using four frequently used *in vitro* procedures (Gamble Solution, simulated lung fluid, simulated epithelial lung fluid and artificial lysosomal fluid). Mouse exposure experiments showed that Pb was mainly distributed in the liver, kidneys, blood and spleen. Based on the kidney model, *in vitro* inhalation bioaccessibility of Pb extracted with optimized Gamble Solution, in which solid to liquid ratio (S/L) was optimized to 1:1000 g ml^{-1} and DTPA was proved to be the key effective component, showed a strong linear relationship with its *in vivo* inhalation bioavailability ($y = 1.07x - 3.86$, $R^2 = 0.73$). Moreover, *in vitro* bioaccessible and bioavailable fractions of Pb were mainly from acid exchangeable and reducible fractions of Pb in $PM_{2.5}$. Altogether, optimized Gamble Solution was suggested for the analysis of *in vitro* bioaccessibility for risk-based assessments.

1. Introduction

Exposure to ambient particulate matter (APM) has been confirmed to be consistently associated with some heart and lung diseases and injuries of the nervous system because of potential harmful matter in APM (e.g., heavy metals, polycyclic aromatic hydrocarbons, microorganisms and endotoxins) (Wang et al., 2017; Kioumourtzoglou et al., 2016; Liu et al., 2018; Goix et al., 2016; Bi et al., 2015). Due to the accumulation of toxic effects to humans, airborne particle-bound heavy metals have received more and more attention (Liu et al., 2018; Goix et al., 2016; Bi et al., 2015; Kastury et al., 2018; Twining et al., 2005; Bierkens et al., 2011; Palus et al., 2003; Navas-Acien et al., 2007). Lead (Pb) is one of the most important heavy metals in APM, and it can lead to high concentrations of lead in blood and urine (Bierkens et al., 2011) and damage to DNA (Palus et al., 2003) and the cardiovascular system (Navas-Acien et al., 2007).

In recent years, the *in vitro* bioaccessibility (BAc, fraction dissolved in a simulated body fluid) and *in vivo* bioavailability (fraction absorbed in the systemic blood circulation) of toxic metals are increasingly examined in health risk assessments (Liu et al., 2018; Goix et al., 2016; Bi et al., 2015; Kastury et al., 2018, 2017). *In vitro* bioaccessibility procedures are low-cost and efficient methods to evaluate exposure risks and are often preferable over *in vivo* bioavailability due to their decreased experimental time, expense and ethical concerns (Kastury et al., 2018). Existing *in vitro* inhalation bioaccessibility procedures, such as Gamble Solution, artificial lysosomal fluid (ALF) (Nemmar et al., 2013), simulated lung fluid (SLF) and simulated epithelial lung fluid (SELF) (Wragg and Klinck, 2007; Boisa et al., 2014; Taunton et al., 2010; Midander et al., 2007), have been used to investigate the bioaccessible fraction of Pb in APM via inhalation exposure. However, these procedures generally lack validation via *in vivo-in vitro* correlation (Kastury et al., 2017). In recent years, the validation of *in vitro* ingestion bioaccessibility procedures via *in vivo-in vitro* correlation has been widely investigated (Denys et al., 2012; Juhasz et al., 2010; Li et al., 2016). The related literature shows that *in vivo* bioavailability can be expressed as absolute bioavailability (ABA) (Schaider et al., 2007) and relative bioavailability (RBA, the ratio of the bioavailability of a certain element in the soil to that of water soluble compound or reference matrix) (Denys et al., 2012; Li et al. (2016); USEPA (2007); Li et al., 2017, 2015; Juhasz et al., 2011). To validate *in vitro* bioaccessibility procedures to predict the *in vivo* RBA of a test element in an environmental material, an empirically strong correlation between *in vivo* and

* Corresponding authors.
E-mail addresses: huxin@nju.edu.cn (X. Hu), hzlian@nju.edu.cn (H.-z. Lian).

https://doi.org/10.1016/j.jhazmat.2019.121202
Received 5 July 2019; Received in revised form 26 August 2019; Accepted 9 September 2019
Available online 12 September 2019
0304-3894/

in vitro data sets is necessary to establish a linear equation (e.g., $RBA = a + b{\cdot}BAc$) (Denys et al., 2012; Li et al. (2016); USEPA (2007); Li et al., 2017, 2015; Juhasz et al., 2011). These studies offer strategies for the validation of *in vitro* inhalation bioaccessibility procedures via *in vivo-in vitro* correlation.

Moreover, the validation of *in vitro* lead bioaccessibility in soils and soil-like materials shows that the physicochemical properties of an environmental medium and the lead species itself are important parameters for BAc and RBA (Kastury et al., 2017; Taunton et al., 2010; Denys et al., 2012; Li et al., 2016, 2017; Li et al., 2015; Juhasz et al., 2011; Moreno Tovar et al., 2012). APM have abundant sources such as suspended soil fine particles, industrial emissions, incineration, and vehicle exhaust (Gummeneni et al., 2011; Kelly and Fussell, 2012; Heo et al., 2017; Zawacki et al., 2018). Therefore, there are different species of lead in APM due to various sources. It is hard to resuspend the collected APM in a sampling membrane; thus, simulated fine particles developed from fine soils/sediments with different levels of lead or spiked lead species are suitable for the related studies.

The *in vivo* inhalation exposure methods in the related literature are generally categorized as inhalation exposure (includes whole-body, head-only, or nose-only exposure) and instillation (IT) methods (including intranasal, intratracheal, intravenous or intraperitoneal) (Kastury et al., 2017). IT methods are simple and operable (Kastury et al., 2017), being more appropriate for an acute exposure model, and an intranasal method was used in this study. Moreover, according to the definition of RBA advocated by Environment Protection Agency, USA (USEPA), spiked soluble lead salt should be used in research of Pb-RBA (USEPA, 2007). To inhalation exposure, it is difficult to produce airborne particles of readily soluble lead for RBA research. However, it is easy for an intranasal method. Therefore, an intranasal method was used in this study.

In the present study, the physicochemical properties of $PM_{2.5}$ containing different lead levels and species were examined using simulated fine soils/sediments containing different levels of lead or spiked lead species. The *in vivo* inhalation bioavailability of lead was investigated through instillation exposure of simulated $PM_{2.5}$ suspension solution. The *in vitro* bioaccessibility of lead was investigated via different *in vitro* procedures. The *in vitro* inhalation bioaccessibility procedures were validated and optimized via *in vivo-in vitro* correlation.

2. Materials and methods

2.1. Sample preparation and characterization

Simulated $PM_{2.5}$ samples contained different levels of Pb were obtained via the ball-milling of collected field surface soils and aged soils spiked with different species of lead compounds. Four soils (surface soil from outlands (SO), sludge near river (SW), surface soil from rice field, and surface dusts from path (SP)) were collected from the Shuikoushan lead-zinc mining area at Hunan, China. The air-dried soils were ground with a pulverizer and then a comet ball grinding mill (QM-3SP2, Nanjing University Instrument Co. LTD) using wet ball-milling with water for 24 h. The sizes of the resulting particles ranged from 0.1 to 1.5 μm and were characterized by using a nanoparticle analyzer (90 Plus, Brookhaven Instruments Corporation), scanning electron microscope (SEM, JEM-2100, JEOL, Ltd.) and X-ray diffractometer (XRD) (see the supplementary information). These resulting $PM_{2.5}$ particles were labeled as SO, SW, SR, and SP. Therefore, simulated $PM_{2.5}$ samples with different physicochemical properties and different levels of Pb were obtained. Moreover, to investigate the influence of Pb species, 7 lead compounds ($PbSO_4$, Pb_3O_4, PbS, $PbCrO_4$, PbO, $PbCO_3$ and $Pb(NO_3)_2$) were spiked into wet surface soil from a vegetable field at Qixia, Nanjing (Pb content: 113 mg kg^{-1}) with ball-milling for 30 min, and then aged for one month. The physicochemical properties of these Pb compounds were presented in Table S1 and the Pb content of spiked simulated $PM_{2.5}$ were 3518–4035 mg kg^{-1} (data were presented in Table S1). The soils were ground as described above after air drying. The resulting particles were characterized as described above and labeled as $PbSO_4$-, Pb_3O_4-, PbS-, $PbCrO_4$-, PbO-, $PbCO_3$- and $Pb(NO_3)_2$-SV. These simulated $PM_{2.5}$ samples were stored in a dryer for the following research.

The total Pb contents and major elements in the simulated $PM_{2.5}$ samples were determined by using an inductively coupled plasma optical emission spectrometer (ICP-OES, Optima 5300, Perkin-Elmer SCIEX) after digestion using the USEPA Method 3050B (USEPA, 1996). Fractionation of Pb in the simulated $PM_{2.5}$ samples were categorized with a modified Community Bureau of Reference (BCR) procedure (details of the modified BCR procedure is presented in the supplementary information) (Huiming et al. (2013); Liu et al. (2017)).

2.2. Animal exposure

The protocols used in this study were approved by the Institutional Animals Care and Use Committee of Nanjing University (Nanjing, China) and were performed in accordance with the National Institutes of Health (NIH) guidelines, as described in the Guide for the Care and Use of Laboratory Animals of the NIH. Eight- to ten-week-old female Balb/c mice were purchased from the Nanjing University Animal Research Centre (Nanjing, China). The mice were housed in pairs in polypropylene cages and allowed to acclimate for 1 week with a 12 -h light/dark cycle (light cycle, 6:00 a.m. to 6:00 p.m.) before the exposure experiments were initiated (temperature, 25 ± 1 °C; humidity, 60%). Food and water were provided *ad libitum*. During the experimental period, the mice were maintained in the same environment. The mean weight of the mice at the start of experiment was 20 ± 2 g. Prior to intranasally instillation, the mice were anesthetized with isoflurane.

2.2.1. Tissue distribution of Pb

Five mice were intranasally instilled with 50 μl of 0.9% sterile saline with PbS-SV suspension at 20 μg μl^{-1}. The mice were euthanized under anesthesia after 48 h culture, and then the whole lung, liver, kidney, spleen, heart, skeletal muscle (from thigh), and blood (0.5 ml) were collected. The muscle and blood were estimated as a percentage of total body weight as 38.4% and 4.9% (Brown et al., 1997), respectively. Mice instilled with sterile saline without PbS-SV were used as controls.

2.2.2. Pb toxicokinetics

Forty mice were intranasally instilled with 50 μl 0.9% sterile saline with PbS-SV suspension at 20 μg μl^{-1}. Five mice were euthanized under anesthesia, and the whole lungs and kidneys were collected at 0, 0.5, 1, 2, 3, 4, 5, 6, and 7 days after treatment. Mice instilled with sterile saline without PbS-SV were used as controls.

2.2.3. Dose-response effects

Three groups of mice (5 mice per group) were intranasally instilled with 50 μl 0.9% sterile saline with lead acetate to achieve a Pb concentration dose of 0, 50, and 100 ng μl^{-1}. After 48 h, the mice were euthanized under anesthesia and the whole liver, kidney, and spleen were collected.

2.2.4. Relative bioavailability

Fifty-five mice were intranasally instilled with 50 μl 0.9% sterile saline with simulated $PM_{2.5}$ sample suspensions at 20 μg μl^{-1}. After 48 h, the mice were euthanized under anesthesia and the whole kidneys were collected. Mice instilled with sterile saline without $PM_{2.5}$ were used as controls.

2.2.5. Suspensions for intranasally instillation

20 μg μl^{-1} simulated $PM_{2.5}$ sample suspensions were made by adding 20 mg solid samples into 1 ml 0.9% sterile saline solution, and then stirring and dispersing with ultrasonic for about 5 min. Prior to intranasally instillation, suspensions were also dispersing with

ultrasonic for about 1 min.

The organ samples were freeze-dried before digestion in concentrated HNO_3 and H_2O_2 at 120 °C until near dryness and then diluted with 0.1 M HNO_3 to 3 ml. The resulting solution was centrifuged (8960 × g for 5 min) and the supernatant were stored in 4 ℃ for analysis.

2.3. Bioaccessibility

In this study, the Gamble Solution, SLF, SELF, and ALF methods were employed. Lead bioaccessibility was determined in triplicate for simulated $PM_{2.5}$. The detailed compositions and parameters for these *in vitro* procedures are outlined in the supplementary information (Table S2).

2.4. Elemental analyses and data treatment

Concentrations of Pb and major elements in the solutions were measured using ICP-OES and inductively coupled plasma mass spectrometry (ICP-MS, Elan9000, Perkin-Elmer SCIEX, USA). The calibration standard solutions (0, 0.1, 0.5, 2.0, 10.0 mg l^{-1} for ICP-OES; 0, 0.5, 2.0, 10.0, 50.0 μg l^{-1} for ICP-MS) were diluted from standard stock solutions (Custom Assurance Standard) purchased from SPEX CertiPreP (1000 mg l^{-1}, Lot number: 28-232CR) containing 2% HNO_3 (V/V). The internal standard solutions (Bi, 20 μg l^{-1}) added on line through a T-junction were diluted from standard stock solutions (Custom Assurance Standard) purchased from SPEX CertiPreP (10 mg l^{-1}, Lot number: CL1-234BIY) containing 2% HNO_3 (V/V). Digested pork liver samples (a Chinese certified reference material, GBW10051) were determined by using the ICP-MS with recovery of 95%, and accuracy of 3%. The relative percent differences in parallel samples were within 20% or the experiments were repeated.

Pb-BAc is the fraction of Pb in simulated $PM_{2.5}$ that could be extracted by simulated body fluid. Pb-RBA is defined as the ratio of Pb content in a certain target organ of the studied mice taken up from the simulated $PM_{2.5}$ to that of water soluble Pb salt (lead acetate, $Pb(AC)_2$). The Pb-RBA and Pb-BAc were then calculated using Eq. (1) (Li et al., 2016) and (2) (Denys et al., 2012), respectively, as follows:

$$RBA(\%) = \left(\frac{kidneyPb_{PM_{2.5}} / kidneyPb_{Pb(Ac)_2}}{Pbdose_{PM_{2.5}} / Pbdose_{Pb(AC)_2}} \right) \times 100\% \quad (1)$$

$$BAc(\%) = \left(\frac{V_l \times C_{Pb} \times d}{m_{PM_{2.5}} \times W_{Pb}} \right) \times 100\% \quad (2)$$

where RBA is the relative bioavailability; kidney $Pb_{PM2.5}$ and kidney $Pb_{Pb(AC)2}$ are the mass of Pb in mouse kidneys exposed to $PM_{2.5}$ and lead acetate (ng), respectively; Pb $dose_{PM2.5}$ and Pb $dose_{Pb(AC)2}$ are the Pb dose levels in mice exposed to simulated $PM_{2.5}$ and Pb acetate (μg), respectively; BAc is the bioaccessibility; V_l is the volume of fluid used in the lung phase extraction including any pH adjustments (Sysalova et al., 2014); C_{Pb} is the measured concentration of Pb in the diluted extract solution (mg l^{-1}); d is the dilution applied to the extract solution prior to analysis; $m_{PM2.5}$ is the mass of $PM_{2.5}$ used in the lung phase extraction (g); and W_{Pb} is the Pb content in simulated $PM_{2.5}$ (mg kg^{-1})

2.5. Statistical analyses

Statistical analyses were performed using SPSS software (version 16). Analysis of variance (independent-sample T test, $p < 0.05$) was used to test the statistically significant differences among the *in vitro* bioaccessibility procedures optimizing. The *in vivo-in vitro* correlation in this study was performed by using Origin (version 9.1).

3. Results and discussion

3.1. Characterization of simulated $PM_{2.5}$

The size of the simulated $PM_{2.5}$ was observed with SEM and dynamic light scattering (Figure S1 and Figure S2). The SEM micrograph showed that the resulting particles were irregular. The dynamic light scattering results showed that the size of the resulting particles ranged from 0.1 to 1.5 μm. Therefore, these particles can be considered as $PM_{2.5}$ from suspended/resuspended fine soil particles.

The lead contents in the simulated $PM_{2.5}$ from Shuikoushan soils were 213–8810 mg kg^{-1} (213 ± 11 for SO, 8810 ± 214 for SW, 1083 ± 15 for SR, and 1151 ± 82 for SP) and 3518–4035 mg kg^{-1} in the simulated $PM_{2.5}$ from the spiked soils. The mapping of Pb and other elements in Figure S1 shows that Fe is associated with Pb in SW. The XRD spectra of SW in Figure S3 shows that the peaks (2θ = 14.9°, 17.4° and 28.9°) for SW were very similar to lead phosphate (2θ = 15.1°, 17.5° and 28.9°) (Qin et al., 2014). The lead-related peaks of other compounds were missing due to the low lead concentrations.

The fractionation of Pb in the simulated $PM_{2.5}$ using modified BCR is presented in Table S3. The recovery of modified BCR ranged from 88.1% to 109.0% (details seen Table S3). The average ratios of the four Pb fractions (the acid exchangeable fractions (F1), the reducible fractions (F2), the oxidizable fractions (F3), and the residual fractions (R)) were approximately 2.2:55.2:25.2:17.4 in SO, 0.01:2.96:2.05:94.98 in SW, 22.52:62.02:8.92:6.54 in SR, 11.24:70.44:8.21:10.12 in SP and 41.07:55.17:2.65:1.11 in PbS-SV. Therefore, different Pb distributions were observed among the simulated particles.

3.2. Inhalation bioavailability of Pb

The relative standard deviation (RSD) of Pb in the lung for 1 h post exposure among 5 mice was 7.3% and the RSD of Pb in the lung in the three batches was below 10% (RSD for the next three batches was 9.3%, 2.6% and 8.1%, n = 5). This means that the mass of instilled $PM_{2.5}$ entering the lungs was controlled and repeatable with the IT method. Lead was mainly distributed in the liver (136.3 ± 18.7 ng), kidneys (110.3 ± 4.5 ng), blood (23.1 ± 5.0 ng), and spleen (2.5 ± 0.4 ng) at 48 h post exposure of the studied mice to PbS-SV suspension solution. Lead in the mouse heart and muscle was below the detected limitations. Gastric-intestinal absorption could be another contribution for Pb absorption into organism from some parts of particles that be cleared from the lungs via mucociliary transport and swallowed. However, the contribution of gastric-intestinal absorption Pb in this experiment was negligible (proving process was presented in SI).

3.2.1. Metabolic kinetics of Pb

Fig. 1 shows the toxicokinetics of Pb in the lungs (a) and kidneys (b) over 7 days of exposure to PbS-SV. The residual Pb in the mouse lungs was approximately 30.0% for 24 h exposure to PbS-SV and 4.5% after 168 h exposure. The mass of Pb in the kidneys rapidly increased during the first 24 h after exposure to PbS-SV and reached a maximum value (134.5 ng) at 24 h of exposure before the mass of Pb decreased slowly to a relatively higher Pb level than the control group Pb level.

Fig. 1a shows that the Pb elimination process in the lungs could be divided into three linear stages as follows: fast elimination stage within 24 h (slope = -59.5; $R^2 = 0.99$), relaxed elimination stage between 24 h to 72 h (slope = -8.9, $R^2 = 0.99$) and slow elimination stage after 72 h (slope = -1.6, $R^2 = 0.92$). The elimination rate of Pb during the first stage in the lungs was approximately 6.7-fold higher than the second stage and 37.2-fold higher than the third stage. This suggested that most of the bioavailable Pb in the simulated $PM_{2.5}$ in the lungs was quickly absorbed in the short-term and the remaining fractions would be eliminated over a long-term period. Similar results have been reported by others researchers studying nanoparticle exposure with the IT method (Konduru et al., 2014; Pang et al., 2016; Molina et al., 2014).

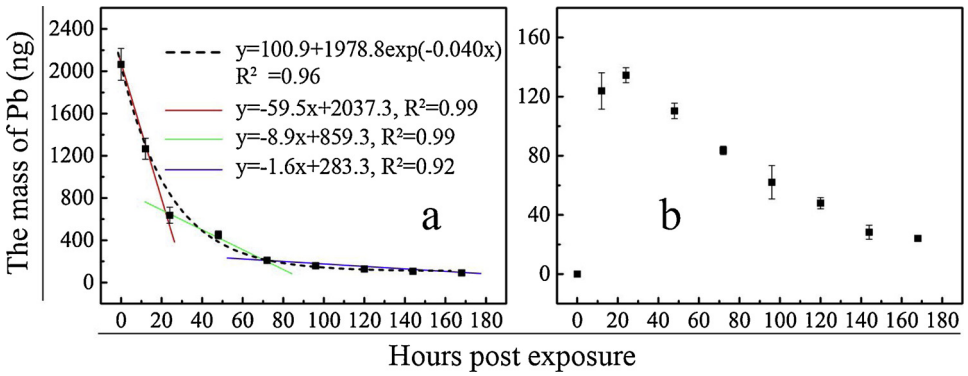

Fig. 1. The metabolic kinetics of Pb in lungs (a) and kidneys (b) during 7-days exposure to PbS-SV.

For example, the clearance of nZnO from rat lungs was rapid, with only 16–18% of the residue present on the 2nd day of exposure, though it took approximately 28 days for the nZnO to be cleared (Konduru et al., 2014). The silver concentration in mouse blood reached a maximum after 1 h exposure to silver nanoparticles and decreased to lower levels after 12 h (Pang et al., 2016). In total, 12% of $nCeO_2$ in rat lungs was cleared on the 1 st day post exposure, and over the following 27 days, only 14% was cleared gradually (Molina et al., 2014). In inhalation studies, the toxicity of the contaminants depends on the duration and intensity of exposure (Phalen et al., 1984), which means that the toxicity of contaminants during the slow intake stage is much less than the fast absorption stage due to its much lower intensity.

In this study, the second stage of Pb elimination in the lungs (24 h–72 h) was a transition stage during which the mass of Pb in the lungs was more stable than the first elimination stage (before 24 h) and higher than the third elimination stage (after 72 h). Therefore, the portion of Pb absorbed within 48 h of exposure was chosen for the calculation of the absolute bioavailable Pb fraction (Pb-ABA_{48h}). The detailed calculation is presented in the supplementary information. The Pb-ABA_{48h} of PbS-SV was approximately 83.4%.

3.2.2. Relative bioavailability

The concentration of Pb in end points at 48 h post exposure was chosen for the study of the RBA as described above. Fig. 2 shows the dose-response curve for Pb by plotting the concentration in the liver (a), kidneys (b) and spleen (c) as a function of the exposure dose. The dose-response in the kidneys and spleen fit well with a linear correlation (R^2 = 0.999 and 0.97, respectively), much better than that in the liver (R^2 = 0.85). However, the proportion of Pb in the kidneys (slope = 0.044) was much higher than that entering the spleen (slope = 0.0015), which resulted in wider range of Pb in the kidneys in the dose-response study. Thus, the dose-response curve in the kidneys was chosen to study the Pb-RBA.

A linear correlation dose-response curve is usually used in oral RBA research, in which the response concentration at an endpoint can reflect an equivalent mass of Pb in soluble salts such as lead acetate (Palus et al., 2003; Damon et al., 1984). Bioavailability of Pb in lead acetate was supposed to be 100% (Palus et al., 2003; Damon et al., 1984). In this research, the content of Pb in the kidneys was linearly dependent to inhalation exposure dose of lead acetate (R^2 = 0.999), which was similar to oral exposure to lead acetate in the kidney (R^2 = 0.98) (Li et al., 2016). This implied that the Pb concentration in the kidneys was linearly related to the bioavailable Pb in the lungs.

The inhalation relative bioavailability of 48 h exposure was generated according to the oral-RBA and described in Eq. (1) (Palus et al., 2003). The Pb-RBA of the 7 simulated $PM_{2.5}$ with different spiked Pb compounds and Shuikoushan soils are presented in Fig. 3. There were great variations among the different $PM_{2.5}$ from aged soils and field soils, suggesting the influence of Pb species in $PM_{2.5}$. The Pb-RBA from the inhalation dose-response curve was almost equal to the Pb-ABA_{48h} for PbS-SV (82.8% and 83.4%, respectively). This implied that the Pb-RBA based on this dose-response curve could also be used to reflect the ABA from inhalation exposure. Thus, the relative bioavailability term could also be used in Pb research through inhalation exposure in the fast-absorbing stage (within 48 h after exposure).

3.3. In vitro inhalation bioaccessibility

The *in vitro* bioaccessibility of Pb (Pb-BAc) in the simulated $PM_{2.5}$ was calculated using Eq. (2) and the results are presented in Table S4. In SLF, the Pb-BAc ranged from 0.005% ($PbCrO_4$-SV) to 0.088% (PbO-SV) for aged soil $PM_{2.5}$ and 0.0006% (SW) to 0.098 for field soil $PM_{2.5}$. In ALF, the Pb-BAc ranged from 0.005% ($PbCrO_4$-SV) to 0.18% ($Pb(NO_3)_2$-SV) for aged soil $PM_{2.5}$ and 0.0004% (SW) to 0.278% for field soil $PM_{2.5}$. In SELF, the Pb-BAc ranged from 0.016% (PbO-SV) to 0.056% ($PbCrO_4$-SV) for aged soil $PM_{2.5}$ and 0.0014% (SW) to 0.298% for field soil $PM_{2.5}$. In Gamble Solution, the Pb-BAc ranged from 16% ($PbCrO_4$-SV) to 19.1% (PbS-SV) for aged soil $PM_{2.5}$ and 1.05% (SW) to 37.96% for field soil $PM_{2.5}$. Large variations in the *in vitro* inhalation bioaccessibility of Pb were found with the different *in vitro* inhalation bioaccessibility procedures.

The bioaccessibility of Pb in APM with *in vitro* inhalation procedures

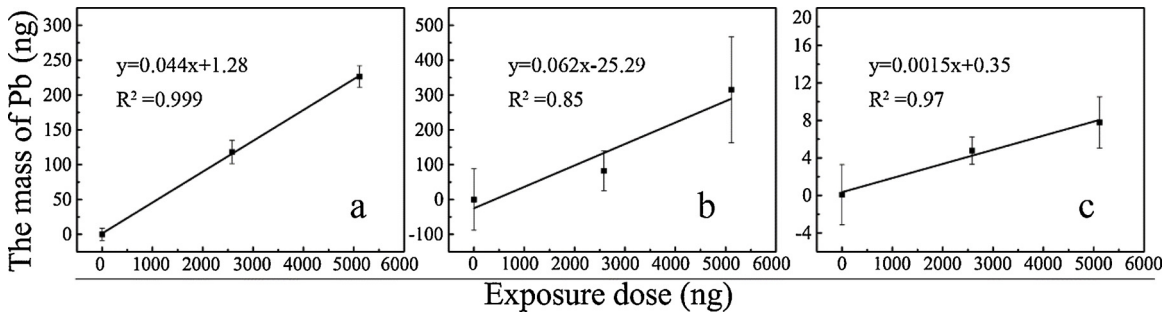

Fig. 2. The dose dependent of Pb in kidneys (a), liver (b) and spleen (c) of mice in 2-days exposure.

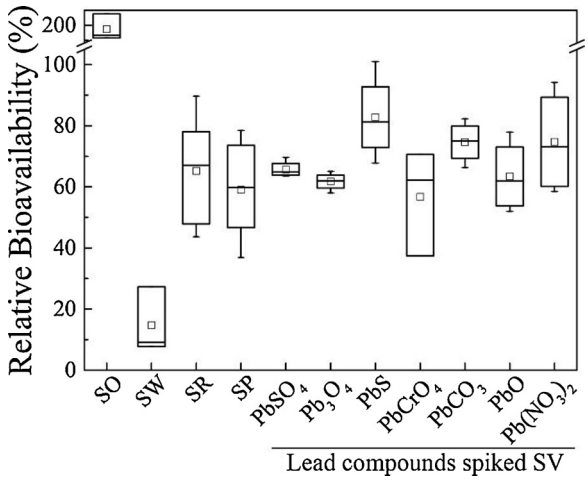

Fig. 3. Range of Pb-RBA in simulated $PM_{2.5}$ (n = 5).

has been reported (Twining et al., 2005; Wragg and Klinck, 2007; Boisa et al., 2014; Sysalova et al., 2014; Hamad et al., 2014; Potgieter-Vermaak et al., 2012; Voutsa and Samara, 2002). Table S5 summarizes the bioaccessibility from related literature. Most *in vitro* inhalation bioaccessibility procedures originate from Gamble Solution (Gamble, 1967). Because of the different conditions used in these studies (such as the sources of samples, the particle size, S/L ratio (S/L, g ml^{-1}) and extraction time), it is hard to compare and analyze the data from different laboratories (Kastury et al., 2017). In this study, the *in vitro* procedures were performed under the same conditions. Therefore, we confidently evaluated and optimized the Pb-BAc from these *in vitro* procedures for predicting the Pb-RBA based on the obtained *in vivo* data.

3.3.1. Screening in vitro procedures via in vivo-in vitro correlation

The relationship between the *in vitro* bioaccessibility of a certain element determined using different *in vitro* bioaccessibility procedures and RBA determined in an animal model assay (e.g., mouse) is usually used to evaluate the abilities of *in vitro* procedures to predict the relative bioavailability of a certain element due to oral exposure. Therefore, the *in vivo-in vitro* correlation of the Pb-BAc for different *in vitro* procedures with Pb-RBA from mice for the simulated $PM_{2.5}$ is shown in Fig. 4. The results show that the Pb-BAc from these *in vitro* procedures was far below the Pb-RBA. The Pb-BAc from Gamble Solution was on the same order of magnitude as the related Pb-RBA and overwhelming greater than the other *in vitro* procedures. In this study,

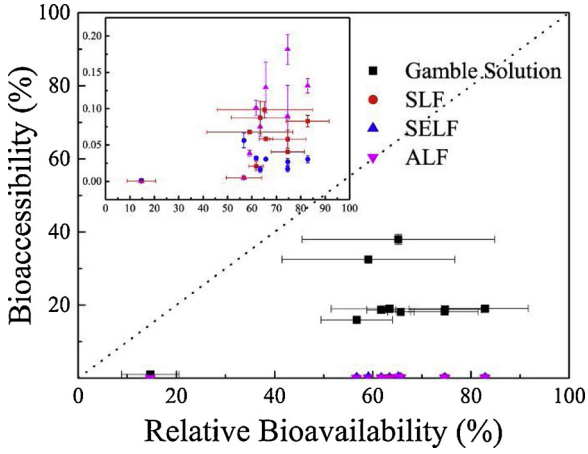

Fig. 4. Plots of BAc with different *in vitro* methods via Pb-RBA (S/L = 1:100 g ml^{-1}).

the operating parameters for Gamble Solution were optimized through the *in vivo-in vitro* correlation to make the Pb-BAc outcomes more confidence.

3.3.2. Effective components in Gamble solution

Fig. 5 shows the influence of albumin, NH_4Cl, cysteine and DTPA (the different ingredients between Gamble Solution and SLF) on SLF for the Pb-BAc of SW, SR and SP. The Pb-BAc of SW, SR and SP were 0.00064%, 0.098% and 0.067% in SLF, respectively. By removing albumin, the Pb-BAc was slightly increased to 0.0016%, 0.14% and 0.11%, respectively. The addition of NH_4Cl and cysteine had no significant influence on the Pb-BAc of SW, SR and SP compared to the removal of albumin from SLF. The Pb-BAc of SW, SR and SP were significantly increased to 0.019%, 45.1% and 39.3% by the addition of DTPA. The results for SR and SP were even higher than the Pb-BAc of Gamble Solution, at 38.0% and 32.5%, respectively. The Pb-BAc of SW upon the addition of DTPA to SLF was less than in Gamble Solution (1.0%).

The Pb-BAc in SLF was lower than in SLF without albumin. This could result from the separation of albumin combined with Pb^{2+} from solution under centrifugation at 8790 *g*. NH_4Cl, cysteine and DTPA are the main components in Gamble Solution. Only the addition of DTPA could significantly improve the Pb-BAc of SLF similar to Gamble Solution levels. This implies that DTPA was the most effective component for extracting Pb. However, DTPA is not contained in biological fluids and many *in vitro* procedures exclude it from their solutions. DTPA was first added to prevent the formation of insoluble phosphate precipitates that might result in an underestimation of yellowcake solubility (Eidson and Mewhinney, 1980). It was also effective for extracting Pb, as is shown in Table S4 in this study. The high Pb-RBA means that the process of extracting Pb from lung fluids is efficient. However, the effective composition in lungs fluids is still unknown. So far, DTPA could be an important substitute.

3.3.3. Optimization of solid to liquid ratios via in vivo-in vitro correlation

Fig. 6a shows the BAc of PbS-SV at different solid to liquid ratios (S/L, g ml^{-1}). It shows that the Pb-BAc increased from 19.1% at an S/L ratio = 1:100 to 67.5% at an S/L ratio = 1:500. It reached the maximum value of 76.1% at an S/L ratio = 1:5000. The RSD of Pb-BAc was below 3.7% when the S/L ratio was greater than 1:5000, but reached 19% at an S/L ratio = 1:10000. Fig. 6b shows the correlation between the Pb-BAc at an S/L ratio = 1:100, 1: 1000 and 1:5000 with Pb-RBA for Pb in simulated $PM_{2.5}$ spiked with Pb compounds. The mean distribution (95% confidence) of the BAc (1:100)-RBA was far below the equivalence line, whereas it was above the equivalence line for BAc (1:5000)-RBA. This value was almost crossed from the ellipse center by the equivalence line for BAc (1:1000)-RBA.

The S/L ratio is an important parameter. First, the S/L ratio parameter is analogous to the mass of APM that an individual breathed in over one day to the volume of lung fluid (Julien et al., 2011). The changeable concentration of $PM_{2.5}$ in an atmosphere environment varies with the physiological environment, resulting in different individual results and a range of data values (S/L ratio: 1:100-1:100,000) (Julien et al., 2011). Thus, S/L ratio has been loosely chosen in many studies (Twining et al., 2005; Wragg and Klinck, 2007; Sysalova et al., 2014; Hamad et al., 2014; Potgieter-Vermaak et al., 2012). Second, there was a lack of *in vivo* data to validate the S/L ratio for *in vitro* inhalation procedures. A few studies have mentioned the importance of the S/L ratio and proven that the S/L ratio could influence the BAc outcome (Kastury et al., 2018; Julien et al., 2011; Pelfrene et al., 2017). However, it was hard to select most appropriate S/L ratio without the *in vivo* data.

In this study, an S/L ratio of 1:5000 resulted in the maximum value of Pb-BAc. This was in agreement with a previous study (Kastury et al., 2018), in which the ratio was chosen as the optimal condition (Kastury et al., 2018). At this ratio, chelators were sufficiently high to extract Pb

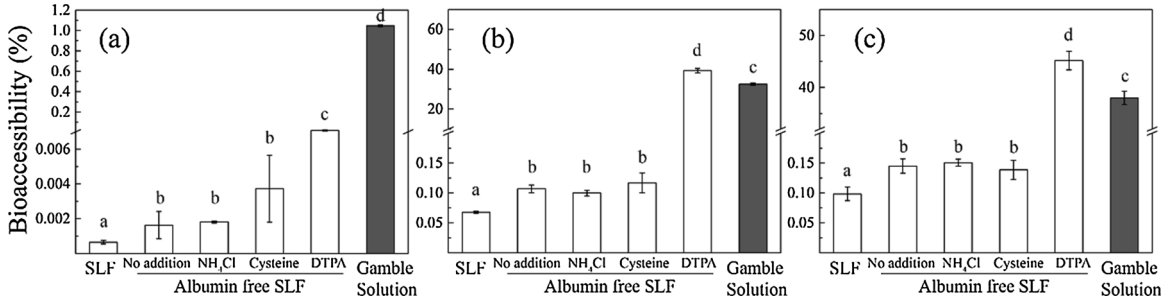

Fig. 5. The influence of albumin, NH_4Cl, cysteine and DTPA to SLF for Pb bioaccessibility of SW (a), SR (b) and SP (c) (S/L = 1:100 g ml^{-1}). The addition of NH_4Cl, Cysteine or DTPA was based on the Albumin free SLF. The different alphabet shows the statistic differences.

and particle agglomeration did not affect Pb dissolution in solution (Kastury et al., 2018). At larger ratios, such as 1:500 or 1:1000, particle agglomeration could decrease the opportunity for Pb in particles to interact with chelators and slightly impaired the dissolution of Pb. At an S/L ratio of 1:100, agglomeration as well as insufficient chelators were the main barrier to Pb dissolution. At the lower ratio of 1:10000, the low concentration of particles allowed higher error in the operation, resulting in a higher outcome RSD (19%). However, the value of Pb-BAc at 1:5000 for Gamble Solution (74–99% for the spiked $PM_{2.5}$) was expected to predict Pb-RBA (56-82% for the spiked $PM_{2.5}$), as is shown in Fig. 6b. The Pb-RBA results suggest that an S/L ratio of 1:1000 for Gamble Solution (66-77%) was optimal. This implied that particle agglomeration could occur in real lung fluids or that a DTPA chelator was the over extraction substitute for the chelators in real lung fluids.

It was worth to mention that results showed that other Pb compounds spiked $PM_{2.5}$ were presented the same high level of Pb-BAc and Pb-RBA with PbS-SV. It implied that all of these Pb compounds were highly and indistinguishably extracted by Gamble Solution or real lung fluids based on the chelating mechanism.

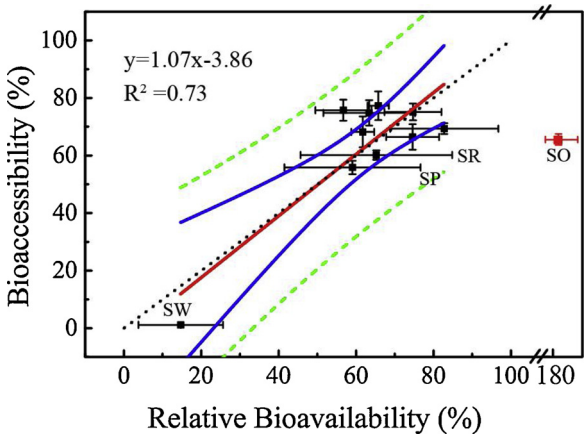

Fig. 7. Plots of BAc (Gamble Solution, S/L ratio: 1:1000 g ml^{-1}) via RBA for Pb in simulated $PM_{2.5}$, The black dotted line is the line of equivalence, the red solid line is correlation line of BAc and against RBA, the blue solid lines are 95% the confidence intervals, and the green dashed lines are the 95% prediction intervals. (For interpretation of the references to colour in this figure legend, the reader is referred to the web version of this article).

3.4. *In vivo-in vitro correlation based on optimized Gamble Solution*

To predict the Pb-RBA of $PM_{2.5}$ via Pb-BAc in Gamble Solution at an S/L ratio of 1:1000, the *in vivo-in vitro* correlation (IVIVC) was established in Fig. 7. The IVIVC curve was plotted based on SP, SR, SW and 7 simulated $PM_{2.5}$ with different spiked Pb compounds, and a linear correlation could be used to fit the experimental data (R^2 = 0.73). The slope of the linear relationship was near to 1 (y = 1.07x – 3.86). SO was excluded when building the relationship for exceeding the Pb-RBA value (180%) and because it was far from the prediction area. The good linear relationship between Pb-BAc and Pb-RBA with a slope close to 1 implied that optimized Gamble Solution at an S/L ratio 1:1000 was a robust *in vitro* procedure to predict the RBA of Pb in the simulated $PM_{2.5}$. It is worth mentioning that the SO value was far above the predicted Pb-RBA; this may have been caused by the low Pb concentration in SO (213 mg kg^{-1}). This implied that a fast exposure model with a single exposure method was not appropriate for studying simulated $PM_{2.5}$ with a low Pb concentration.

3.5. *Relationship between the fractionation of lead and BAc or RBA*

Table S5 shows the relationship between the Pb-BAc (Gamble Solution at an S/L ratio 1:1000) or Pb-RBA and the Pb fractions from the sum of the acid exchangeable fractions, reducible fractions or oxidizable fractions (e.g., F1 + F2+F3 and F1 + F2). The Pb-BAc or Pb-RBA showed a better linear relationship with F1 + F2 (R^2 = 0.997 or 0.94, respectively) than with F1 + F2+F3 (R^2 = 0.98 or 0.89, respectively) (Fig. 8). Figure S5a shows that the Pb-BAc of $PM_{2.5}$ was below the A + R proportion. Fig. 8b shows that the Pb-RBA of $PM_{2.5}$ was below the F1 + F2 proportion, except in SW. In SW, Pb appears to be

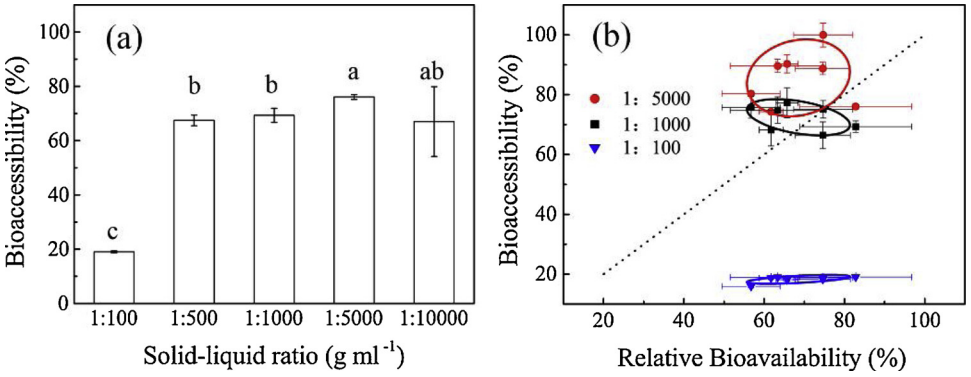

Fig. 6. The BAc of Pb from Gamble Solution at different solid to liquid ratio (a) and their correlations with Pb-RBA in the corresponding $PM_{2.5}$ (b). The black dotted line is the line of equivalence. The solid red, black and blue line are the mean distribution area of the points at 95% confidence. (For interpretation of the references to colour in this figure legend, the reader is referred to the web version of this article).

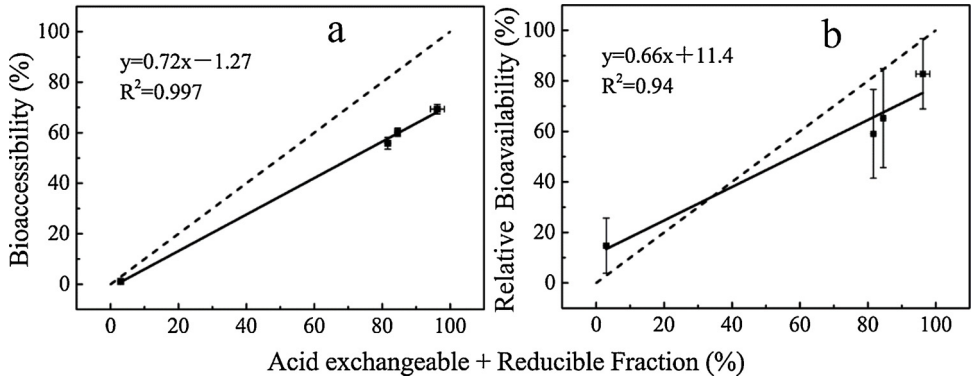

Fig. 8. Correlation plots of BA (a) or RBA (b) against the sum of Acid exchangeable fraction and reducible fraction (F1 + F2) of Pb by BCR method in $PM_{2.5}$. The black dashed line is the line of equivalence.

associated with iron oxide and phosphate minerals as described above, and consequently has a low proportion in F1 + F2 (Moreno Tovar et al., 2012). The proportion of F1 + F2 was similar to Pb-BAc but less than Pb-RBA. This implied that the hard dissolved Pb fraction would potentially be partly extracted by lung fluids, and both the Pb-BAc and proportion of F1 + F2 would underestimate Pb-RBA in the simulated $PM_{2.5}$.

The F1 + F2 or F1 + F2+F3 of Pb in the simulated $PM_{2.5}$ was usually used to substitute for the bioavailable fractions in some studies (Julien et al., 2011). This study proved that the Pb-BAc or Pb-RBA of the simulated $PM_{2.5}$ was more closely related to the F1 + F2 fractions. However, as shown in Fig. 8, the greater proportion of F1 + F2 was higher than Pb-BAc or Pb-RBA in SP, SR and PbS-SV. In the simulated $PM_{2.5}$ with high Pb-BAc or Pb-RBA, the proportion of F1 + F2 appears to overestimate Pb-BAc or Pb-RBA. Altogether, the acid exchangeable and reducible fractions were the main source for the bioaccessible and bioavailable fractions of Pb.

4. Conclusion

Great variations on the *in vitro* inhalation bioaccessibility of Pb in $PM_{2.5}$ were observed among four *in vitro* procedures (Gamble Solution, SLF, SELF and ALF). Gamble Solution was selected among four *in vitro* procedures via *in vivo-in vitro* correlation. The comparisons of components of *in vitro* procedures revealed that DTPA was a key component for Pb extraction and 1:1000 (g ml^{-1}) was the optimized S/L ratio for Pb-BAc. Based on an optimized Gamble Solution, the *in vivo-in vitro* correlation showed good performance for the prediction of RBA. Correlation analysis showed that the acid exchangeable and reducible fractions of Pb in $PM_{2.5}$ were the main sources of *in vitro* bioaccessible and bioavailable Pb. Therefore, optimized Gamble Solution was suggested for the analysis of *in vitro* bioaccessibility for risk-based assessment.

Acknowledgments

We gratefully acknowledge financial support from the National Natural Science Foundation of China (91543129 and 91643105) and the Natural Science Foundation of Jiangsu Province, China (BK20181261).

Appendix A. Supplementary data

Supplementary material related to this article can be found, in the online version, at doi:https://doi.org/10.1016/j.jhazmat.2019.121202.

References

Bi, X.Y., Li, Z.G., Sun, G.Y., Liu, J.L., Han, Z.X., 2015. In vitro bioaccessibility of lead in surface dust and implications for human exposure: a comparative study between industrial area and urban district. J. Hazard. Mater. 297, 191–197.
Bierkens, J., Smolders, R., Van Holderbeke, M., Cornelis, C., 2011. Predicting blood lead levels from current and past environmental data in Europe. Sci. Total Environ. 409 (23), 5101–5110.
Boisa, N., Elom, N., Dean, J.R., Deary, M.E., Bird, G., Entwistle, J.A., 2014. Development and application of an inhalation bioaccessibility method (IBM) for lead in the PM10 size fraction of soil. Environ. Int. 70, 132–142.
Brown, R.P., Delp, M.D., Lindstedt, S.L., Rhomberg, L.R., Beliles, R.P., 1997. Physiological parameter values for physiologically based pharmacokinetic models. Toxicol. Ind. Health 13 (4), 407–484.
Damon, E.G., Eidson, A.F., Hahn, F.F., Griffith, W.C., Guilmette, R.A., 1984. Comparison of early lung clearance of yellowcake aerosols in rats with in vitro dissolution and Ir analysis. Health Phys. 46 (4), 859–866.
Denys, S., Caboche, J., Tack, K., Rychen, G., Wragg, J., Cave, M., Jondreville, C., Feidt, C., 2012. In vivo validation of the unified BARGE method to assess the bioaccessibility of arsenic, antimony, cadmium, and lead in soils. Environ. Sci. Technol. 46 (11), 6252–6260.
Eidson, A.F., Mewhinney, J.A., 1980. In vitro solubility of yellowcake samples from four Uranium mills and the implications for bioassay interpretation. Health Phys. 39, 893–902.
Gamble, J.L., 1967. Chemical Anatomy, Physiology and Pathology of Extracellular Fluid: a Lecture Syllabus. Harvard University Press.
Goix, S., Uzu, G., Oliva, P., Barraza, F., Calas, A., Castet, S., Point, D., Masbou, J., Duprey, J.L., Huayta, C., Chincheros, J., Gardon, J., 2016. Metal concentration and bioaccessibility in different particle sizes of dust and aerosols to refine metal exposure assessment. J. Hazard. Mater. 317, 552–562.
Gummeneni, S., Bin Yusup, Y., Chavali, M., Samadi, S.Z., 2011. Source apportionment of particulate matter in the ambient air of Hyderabad city, India. Atmos. Res. 101 (3), 752–764.
Hamad, S.H., Schauer, J.J., Shafer, M.M., Abd Al-Rheem, E., Skaar, P.S., Heo, J., Tejedor-Tejedor, I., 2014. Risk assessment of total and bioavailable potentially toxic elements (PTEs) in urban soils of Baghdad-Iraq. Sci. Total Environ. 494, 39–48.
Heo, J., Wu, B., Abdeen, Z., Qasrawi, R., Sarnat, J.A., Sharf, G., Shpund, K., Schauer, J.J., 2017. Source apportionments of ambient fine particulate matter in Israeli, Jordanian, and Palestinian cities. Environ. Pollut. 225, 1–11.
Huiming, L.I., Qian, X., Wei, H.U., Wang, Y., Gao, H., 2013. Chemical speciation and human health risk of trace metals in urban street dusts from a metropolitan city, Nanjing, SE China. Sci. Total Environ. 456-457 (7), 212–221.
Juhasz, A.L., Weber, J., Naidu, R., Gancarz, D., Rofe, A., Todor, D., Smith, E., 2010. Determination of cadmium relative bioavailability in contaminated soils and its prediction using in vitro methodologies. Environ. Sci. Technol. 44 (13), 5240–5247.
Juhasz, A.L., Weber, J., Smith, E., 2011. Influence of saliva, gastric and intestinal phases on the prediction of As relative bioavailability using the Unified Bioaccessibility Research Group of Europe Method (UBM). J. Hazard. Mater. 197, 161–168.
Julien, C., Esperanza, P., Bruno, M., Alleman, L.Y., 2011. Development of an in vitro method to estimate lung bioaccessibility of metals from atmospheric particles. J. Environ. Monit. 13 (3), 621–630.
Kastury, F., Smith, E., Juhasz, A.L., 2017. A critical review of approaches and limitations of inhalation bioavailability and bioaccessibility of metal(loid)s from ambient particulate matter or dust. Sci. Total Environ. 574, 1054–1074.
Kastury, F., Smith, E., Karna, R.R., Scheckel, K.G., Juhasz, A.L., 2018. An inhalation-ingestion bioaccessibility assay (IIBA) for the assessment of exposure to metal(loid)s in PM10. Sci. Total Environ. 631-632, 92–104.
Kelly, F.J., Fussell, J.C., 2012. Size, source and chemical composition as determinants of toxicity attributable to ambient particulate matter. Atmos. Environ. 60, 504–526.
Kioumourtzoglou, M.A., Schwartz, J.D., Weisskopf, M.G., Melly, S.J., Wang, Y., Dominici, F., Zanobetti, A., 2016. Long-term PM2.5 exposure and neurological hospital admissions in the northeastern United States. Environ. Health Perspect. 124 (1), 23–29.
Konduru, N.V., Murdaugh, K.M., Sotiriou, G.A., Donaghey, T.C., Demokritou, P., Brain,

J.D., Molina, R.M., 2014. Bioavailability, distribution and clearance of tracheally-instilled and gavaged uncoated or silica-coated zinc oxide nanoparticles. Part. Fibre Toxicol. 11 (1), 44.
Li, J., Li, K., Cave, M., Li, H.B., Ma, L.Q., 2015. Lead bioaccessibility in 12 contaminated soils from China: correlation to lead relative bioavailability and lead in different fractions. J. Hazard. Mater. 295, 55–62.
Li, H.B., Zhao, D., Li, J., Li, S.W., Wang, N., Juhasz, A.L., Zhu, Y.G., Ma, L.Q., 2016. Using the SBRC assay to predict lead relative bioavailability in urban soils: contaminant source and correlation model. Environ. Sci. Technol. 50 (10), 4989–4996.
Li, S.W., Liu, X., Sun, H.J., Li, M.Y., Zhao, D., Luo, J., Li, H.B., Ma, L.N.Q., 2017. Effect of phosphate amendment on relative bioavailability and bioaccessibility of lead and arsenic in contaminated soils. J. Hazard. Mater. 339, 256–263.
Liu, B., Ai, S., Zhang, W., Huang, D., Zhang, Y., 2017. Assessment of the bioavailability, bioaccessibility and transfer of heavy metals in the soil-grain-human systems near a mining and smelting area in NW China. Sci. Total Environ. 609, 822–829.
Liu, R.Y., He, R.W., Cui, X.Y., Ma, L.N.Q., 2018. Impact of particle size on distribution, bioaccessibility, and cytotoxicity of polycyclic aromatic hydrocarbons in indoor dust. J. Hazard. Mater. 357, 341–347.
Midander, K., Pan, J., Wallinder, I.O., Leygraf, C., 2007. Metal release from stainless steel particles in vitro - influence of particle size. J. Environ. Monit. 9 (1), 74–81.
Molina, R.M., Konduru, N.V., Jimenez, R.J., Pyrgiotakis, G., Demokritou, P., Wohlleben, W., Brain, J.D., 2014. Bioavailability, distribution and clearance of tracheally in-stilled, gavaged or injected cerium dioxide nanoparticles and ionic cerium. Environ. Sci. Nano 1 (6), 561–573.
Moreno Tovar, R., Tellez Hernandez, J., Monroy Fernandez, M.G., 2012. Influence of minerals from the tailings in the bioaccessibility of arsenic, lead, zinc and cadmium, in the mining district Zimapan, Mexico. Rev. Int. De Contam. Ambie 28 (3), 203–218.
Navas-Acien, A., Guallar, E., Silbergeld, E.K., Rothenberg, S.J., 2007. Lead exposure and cardiovascular disease - a systematic review. Environ. Health Perspect. 115 (3), 472–482.
Nemmar, A., Holme, J.A., Rosas, I., Schwarze, P.E., Alfaro-Moreno, E., 2013. Recent advances in particulate matter and nanoparticle toxicology: a review of the in vivo and in vitro studies. Biomed Res. Int., 279371.
Palus, J., Rydzynski, K., Dziubaltowska, E., Wyszynska, K., Natarajan, A.T., Nilsson, R., 2003. Genotoxic effects of occupational exposure to lead and cadmium. Mutat. Res. Gen. Toxicol. Environ. 540 (1), 19–28.
Pang, C.F., Brunelli, A., Zhu, C.H., Hristozov, D., Liu, Y., Semenzin, E., Wang, W.W., Tao, W.Q., Liang, J.N., Marcomini, A., Chen, C.Y., Zhao, B., 2016. Demonstrating ap-proaches to chemically modify the surface of Ag nanoparticles in order to influence their cytotoxicity and biodistribution after single dose acute intravenous adminis-tration. Nanotoxicology 10 (2), 129–139.
Pelfrene, A., Cave, M.R., Wragg, J., Douay, F., 2017. In vitro investigations of human bioaccessibility from reference materials using simulated lung fluids. Int. J. Environ. Res. Public Health 14 (2), 112.
Phalen, R.F., Mannix, R.C., Drew, R.T., 1984. Inhalation exposure methodology. Environ. Health Perspect. 56 (June), 23–34.
Potgieter-Vermaak, S., Rotondo, G., Novakovic, V., Rollins, S., Van Grieken, R., 2012. Component-specific toxic concerns of the inhalable fraction of urban road dust. Environ. Geochem. Health 34 (6), 689–696.
Qin, F., Wu, X., Zhai, S.M., Qin, S., Yang, K., Chen, D.L., Li, Y.C., 2014. Pressure-induced phase transition of lead phosphate $Pb_3(PO_4)_2$: X-ray diffraction and XANES. Phase Transit. 87 (12), 1255–1264.
Schaider, L.A., Senn, D.B., Brabander, D.J., McCarthy, K.D., Shine, J.P., 2007. Characterization of zinc, lead, and cadmium in mine waste: implications for trans-port, exposure, and bioavailability. Environ. Sci. Technol. 41 (11), 4164–4171.
Sysalova, J., Szakova, J., Tremlova, J., Kasparovska, K., Kotlik, B., Tlustos, P., Svoboda, P., 2014. Methodological aspects of in vitro assessment of bio-accessible risk element pool in urban particulate matter. Biol. Trace Elem. Res. 161 (2), 216–222.
Taunton, A.E., Gunter, M.E., Druschel, G.K., Wood, S.A., 2010. Geochemistry in the lung: reaction-path modeling and experimental examination of rock-forming minerals under physiologic conditions. Am. Mineral. 95 (11–12), 1624–1635.
Twining, J., McGlinn, P., Loi, E., Smith, K., Giere, R., 2005. Risk ranking of bioaccessible metals from fly ash dissolved in simulated lung and gut fluids. Environ. Sci. Technol. 39 (19), 7749–7756.
USEPA, 1996. Method 3050B: Acid Digestion of Sediments, Sludges, and Soils. United States Environmental Protection Agency. http://www.epa.gov/wastes/hazard.
USEPA, 2007. Guidance for Evaluating the Oral Bioavailability of Metals in Soils for Use in Human Health Risk Assessment. United States Environmental Protection Agency. https://www.epa.gov/superfund.
Voutsa, D., Samara, C., 2002. Labile and bioaccessible fractions of heavy metals in the airborne particulate matter from urban and industrial areas. Atmos. Environ. 36 (22), 3583–3590.
Wang, J.D., Xing, J., Mathur, R., Pleim, J.E., Wang, S.X., Hogrefe, C., Gan, C.M., Wong, D.C., Hao, J.M., 2017. Historical trends in PM2.5-related premature mortality during 1990-2010 across the northern Hemisphere. Environ. Health Perspect. 125 (3), 400–408.
Wragg, J., Klinck, B., 2007. The bioaccessibility of lead from Welsh mine waste using a respiratory uptake test. J. Environ. Sci. Health A 42 (9), 1223–1231.
Zawacki, M., Baker, K.R., Phillips, S., Davidson, K., Wolfe, P., 2018. Mobile source con-tributions to ambient ozone and particulate matter in 2025. Atmos. Environ. 188, 129–141.